

# APPLICATION OF PURE CERIA AND COPPER-CERIA ELECTROSPUN NANOFIBER IN THE WATER GAS SHIFT REACTION

D. B. Pal<sup>1</sup>, R. Chand<sup>2</sup>, P. Singh<sup>3</sup>, P. K. Mishra<sup>4</sup>

<sup>1,4</sup>Department of Chemical Engineering and Technology, Indian Institute of Technology (BHU), Varanasi U.P., (India)

<sup>2</sup>Department of Chemical Engineering, National Institute of Technology, Rourkela, Odisha, (India)

<sup>3</sup>Department of Chemistry, Indian Institute of Technology (BHU), Varanasi, U.P., (India)

## ABSTRACT

Pure CeO<sub>2</sub> and 20 mol. % Cu/CeO<sub>2</sub> composite nanofibers were fabricated by using Electrospinning method. Copper acetate monohydrate and cerium nitrate hexahydrate were used as the inorganic precursors, PVP was used as the guiding polymer and the electrospinning was carried out at 12kV DC voltage by maintaining a tip to collector distance of 10 cm. The synthesized nanofibers were characterized by SEM and EDX analysis and the average diameters of pure ceria and 20 mol. % Cu/CeO<sub>2</sub> nanofibers were found to be 130 nm and 117 nm (both before calcination), respectively. After calcination for 3 hours, the fiber diameters were reduced by around 30-40% due to the removal of organic compounds present in the nanofiber mats. The crystal structure of the nanofibers was determined by X-ray diffraction (XRD) technique. The most intense peak of CeO<sub>2</sub> was observed at a two-theta value of 27.84° and the average crystallite sizes of CeO<sub>2</sub> and 20 mol. % Cu/CeO<sub>2</sub> were calculated to be 12 nm and 9 nm, respectively. At 320°C, the nanofibers of 20 mol. % Cu/CeO<sub>2</sub> exhibited superior catalytic activity (61%CO conversion ~) compared to pure CeO<sub>2</sub> nanofibers (57%CO conversion ~). The catalytic activities were maintained up to 370 °C in both the cases to ascertain their applicability in water gas shift reaction.

**Keywords:** Ceria, Carbon Monoxide, Electrospinning, Hydrogen, Nanofibers, Water Gas Shift Reaction.

## I. INTRODUCTION

Hydrogen has tremendous applications in various domestic and industrial sectors [1]. Hydrogen is used in petroleum refining [2, 3], ammonia synthesis via Haber-Bosch process [4], refining of various metals [5, 6], and has many more applications. Hydrogen is also preferred as a source of 'clean' energy due to its high mass-based energy density and the fact that it doesn't lead to emission of harmful gases when burnt [7]. Currently, steam reforming is the most widely method to produce hydrogen [8]. This method involves reacting methane and steam to produce H<sub>2</sub> and carbon monoxide (CO). Using this gaseous mixture in fuel cells leads to the poisoning of platinum electrodes due to the presence of CO [9-11]. Therefore, the undesirable CO must be removed from the gaseous mixture by implementing a follow-up technique known as the Water Gas Shift Reaction. The water

gas shift reaction (WGS) is an important process to produce CO-free hydrogen or to adjust the H<sub>2</sub>/CO ratio [12]. Suitable catalysts, having the desirable properties, have been developed over the years to aid the reaction. In recent years, ceria-based Water Gas Shift (WGS) catalysts have been investigated in lot of detail because of their elevated oxygen transport capacity and the ability to easily switch between reduced and oxidized states [13]. Synthesizing ceria-based nano-catalysts in the form of nanofibers, nanobelts, nanoribbons, nanowires, etc. can further enhance the activity of conventional ceria-based WGS catalysts. Nanofibers may be fabricated by using methods such as phase separation [14], template synthesis [15], electrospinning [16], etc. Among these methods, Electrospinning is considered to be the most suitable for synthesis of nanofibers. Electrospinning produces continuous nanofibers and provides increased ease of fiber production and better flexibility [17]. Moreover, electrospinning allows for better control over fiber diameter, microstructure and arrangement [18, 19].

The aim of the present work is to study the synthesis of pure ceria (CeO<sub>2</sub>) and Cu/CeO<sub>2</sub> composite nanofibers having 20 mol. % Cu (copper-ceria basis) by the electrospinning technique for possible use as catalysts in the Water Gas Shift Reaction. Pure ceria and Cu/CeO<sub>2</sub> composite nanofibers were synthesized by using Cerium nitrate hexahydrate and Copper acetate monohydrate as inorganic precursors.

## II. EXPERIMENTAL

### 2.1. Preparation of the spinning solution

Cerium nitrate hexahydrate (Ce(NO<sub>3</sub>)<sub>3</sub>.6H<sub>2</sub>O) and cupric acetate monohydrate (Cu(CH<sub>3</sub>COO)<sub>2</sub>.H<sub>2</sub>O) precursors were used for the process. Polyvinyl pyrrolidone (PVP) was used as the guiding polymer for preparing the spinning solution. Ethanol and de-ionized water were selected as the solvent and co-solvent, respectively. Glacial acetic acid was employed as the reducing agent.

Two different solutions were prepared - pure ceria and 20 mol. % Cu. For each case, 12 ml of spinning solution was prepared. 8 ml of ethanol and 4 ml of de-ionized water were taken in separate vials (ethanol: water = 2: 1). The 10% w/v (1.2 g) PVP was added to the vial containing ethanol and was magnetically stirred. After that, 0.434 g of Ce(NO<sub>3</sub>)<sub>3</sub>.6H<sub>2</sub>O and 0.05 g (20 mol% Cu) of Cu(CH<sub>3</sub>COO)<sub>2</sub>.H<sub>2</sub>O were added to the vial containing water. The contents of both the vials were mixed together and 2-3 drops of acetic acid was added to the final solution. The mixed solution was then magnetically stirred for 3 hours at room temperature to form a homogeneous solution. For preparing casting solution for pure ceria nanofibers, above procedure was followed but no Cu(CH<sub>3</sub>COO)<sub>2</sub>.H<sub>2</sub>O was added.

### 2.2. Preparation of electrospun nanofiber

The basic electrospinning setup consists of a high-voltage power supply (preferably DC), a syringe pump, a blunt metallic needle and a conductive collector plate. The details of the set have been described elsewhere [20]. The precursor solution was filled in a 6 ml plastic syringe equipped with a stainless steel flat-tip needle (21 gauge). The syringe was attached to the syringe pump and the system was arranged vertically. The syringe pump was configured to pump out the spinning solution at 1ml/hr. The metallic collector plate was kept directly under the needle tip to collect the nanofibers. The distance between the syringe tip and the collector plate was maintained at 10 cm. A high DC voltage of about 12 kV was provided between the needle tip and the collector. The experiment was carried out in air (65% relative humidity) and at room temperature. The electrospun

nanofibers were finally collected and calcined in air at 500<sup>0</sup>C for 3 hours to obtain Cu/CeO<sub>2</sub> nanofibers. The calcined nanofibers were subsequently cooled and subjected to morphological characterization.

### **2.3 Catalytic reaction**

The overall experimental setup consisted of four sections: feed section, reactor, product cooling and separation unit. The CO and N<sub>2</sub> are fed from respective cylinders using flow measuring device, mercury safety device and water vapor-generating sparger. Reaction system consisted of a compact bench scale tubular reactor, a tubular furnace and a micro-processor based temperature controller. After the completion of reaction, the products were sent to the cooling section and ultimately to gas-liquid separating systems.

A quartz-tube reactor was employed in which 100 mg of the catalyst was packed over the glass wool. The reactions were carried out at atmospheric pressure and in the temperature range of 150-360<sup>0</sup>C. A J-type thermocouple was inserted into the centre of the catalyst bed to monitor the reaction temperature. The feed consisted of a mixture of 1.5 ml/min. of CO and 58.5 ml/min of N<sub>2</sub>. The gas mixture was divided into two parts - primary and secondary. Feed water vapour was generated at a controlled rate of 0.15 ml/h (as a liquid) by bubbling the secondary part of the gas mixture through a fine epidermis needle in water sparser burette. The primary gas and the secondary gas (along with water vapour) were again mixed before entering into the reactor. The level of water in the sparser burette was constantly maintained by filling it after vaporization of every 1ml of liquid water. This was done to maintain a constant rate of water vapour generation. The catalyst bed temperature was maintained at the desired temperature with the help of a microprocessor temperature controller. The temperature was varied from 150 to 400<sup>0</sup>C and the reactor effluent was analyzed by an on-line gas chromatograph (NUCON-5765).

The reaction products were taken out from the bottom of the reactor and were sent to a condenser and gas-liquid separating assembly kept in an ice-bath to remove water from the mixture before gas-chromatography analysis can be carried out. A porapak Q column, methanizer and FID were used to analyze CO and CO<sub>2</sub>. On the other hand, Molecular sieve column and TCD were used to analyze H<sub>2</sub>.

## **III. RESULTS AND DISCUSSION**

### **3.1. Scanning Electron Microscopy Analysis (SEM)**

The morphologies of the electrospun nanofibers were analyzed with the help of a scanning electron microscope (SEM). Fig.1 shows the SEM images of pure ceria electrospun nanofibers (a) before and (b) after calcination. Fig.2 shows the SEM images of 20 mol. % Cu/CeO<sub>2</sub> electrospun nanofibers (a) before and (b) after calcination. Pure ceria nanofibers were found to have an average diameter of about 130 nm (Fig.1a). On the other hand, the average diameter of the 20 mol. % Cu/CeO<sub>2</sub> nanofibers was found to be approximately 117 nm (Fig.2a). After calcination, the average diameters got reduced to about 30-40 % of the initial values due to the loss of PVP and other organic compounds during calcination. After calcination, the diameter of the 20 mol. % Cu/CeO<sub>2</sub> nanofibers was found to be 79 nm (Fig.2b). On the other hand, the diameter of pure ceria nanofibers was reduced to 98 nm (Fig.1b).

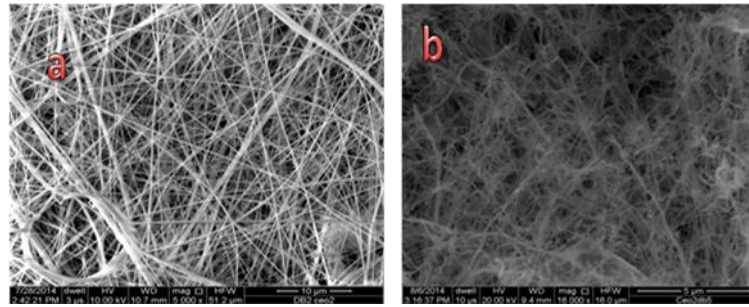


Fig. 1. SEM images of pure ceria nanofiber (a) before and (b) after calcinations.

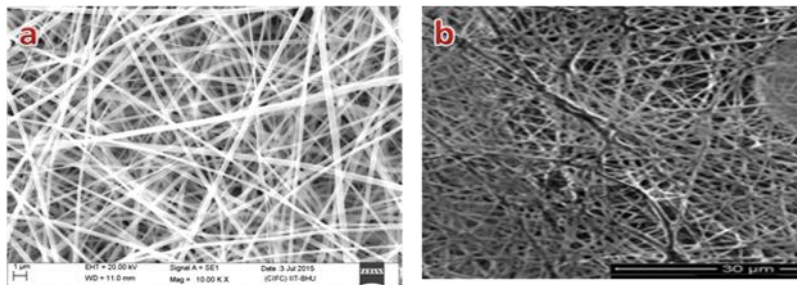


Fig. 2. SEM images of 20 mol. % Cu/CeO<sub>2</sub> nanofibers (a) before and (b) after calcinations.

### 3.2 Energy Dispersive X-Ray Spectroscopy (EDX) Analysis:

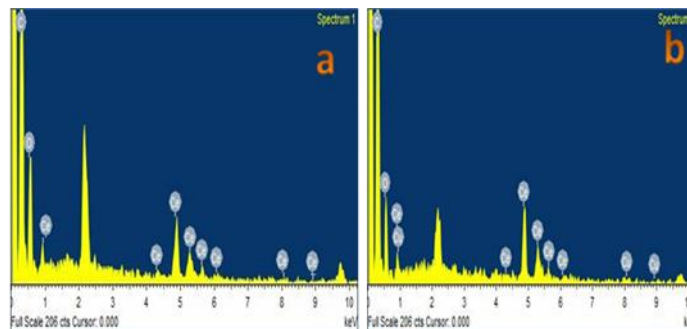


Fig. 3. EDX of nanofiber containing a) pure CeO<sub>2</sub> and b) 20 mol. % Cu/CeO<sub>2</sub>

The atomic compositions of the synthesized nanofibers were estimated using an Energy Dispersive X-Ray Spectroscopy system (EDX; X-ACT 51-ADD0048, OXFORD INSTRUMENTS). Fig. 3a and 3b show the EDAX finger-print of the synthesized nanofibers (pure CeO<sub>2</sub> and 20 mol % Cu/CeO<sub>2</sub>, respectively) prior to calcinations. From Fig. 3a, it is seen that the synthesized nanofibers do not contain any copper, thus confirming the formation of pure ceria nanofibers. Similarly, from Fig. 3b it is seen that the nanofibers contain 0.44% Cu and 1.21% Ce, which translates into a copper-cerium (Cu/[Cu + Ce]) mole fraction ratio of roughly 0.267 (~0.2), thereby confirming the formation of 20 mol. % Cu/CeO<sub>2</sub> nanofibers. These results also confirm that Cu was uniformly distributed in the casting solution.

### 3.3 X-Ray Diffraction Analysis

XRD data was recorded by an 18KW rotating anode based powder diffractometer (Rigaku, Japan) the diffractometer operated at 40kV and 150MA. Powder XRD data were collected in the two-theta range 20-80°. The scan rate was specified as 2 degrees/minute and the scan step was set as 0.02 degree. The diffraction

patterns have been indexed by comparison with the JCPDS files. The XRD patterns of the  $\text{CeO}_2$  and 20 mol. %  $\text{Cu/CeO}_2$  nanofibers are presented in Fig. 4. The graph exhibits peaks which are characteristic of a fluorite-like cubic phase. The most intense peaks of  $\text{CeO}_2$  are clearly visible at  $2\theta$  values of  $28.74^\circ$  and  $47.24^\circ$ , and the average crystallite sizes of  $\text{CeO}_2$  and 20 mol. %  $\text{Cu/CeO}_2$  were calculated by Debye Scherer formula to be equal to 12 nm and 9 nm, respectively.

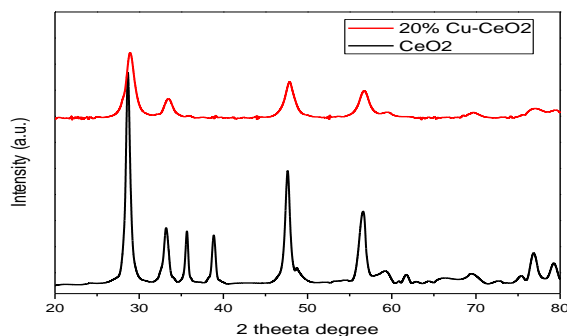


Fig.4. XRD of  $\text{CeO}_2$  & 20 mol. %  $\text{Cu/CeO}_2$  nanofiber calcined at  $500^\circ\text{C}$  for 3hrs.

### 3.4 Fourier Transforms Infrared Spectroscopy

The functional group analysis of the prepared nanofibers was carried out by an FTIR spectrometer. Nanofibers were mixed in KBr pellets and were scanned in the range of  $400\text{-}1400\text{ cm}^{-1}$  for 16 times and the resulting spectrum was recorded. The FTIR spectra of  $\text{CeO}_2$  and 20 mol. %  $\text{Cu/CeO}_2$  nanomaterials are shown in Fig. 5.

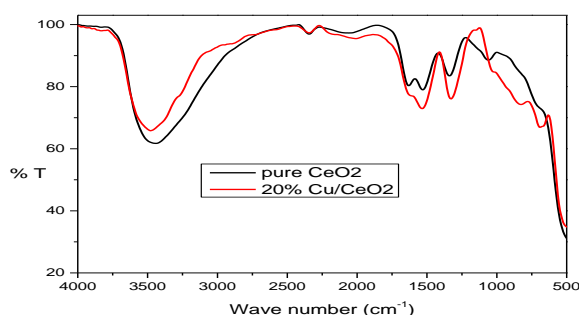


Fig. 5. FTIR spectra of  $\text{CeO}_2$  & 20 mol. %  $\text{Cu/CeO}_2$  nanofibers calcined at  $500^\circ\text{C}$  for 3hrs.

The stretching vibration of the hydroxyl (OH) group of chemisorbed water gives rise to a broad band ( $3700\text{ to }3000\text{ cm}^{-1}$ ). The disappearance of peak ( $900\text{-}1630\text{ cm}^{-1}$ ) after calcination of  $\text{CeO}_2$  at  $500^\circ\text{C}$  indicates the removal of most of the organic compounds present in the nanofiber mats. The formation of  $\text{CeO}_2$  nanofibers is represented by the significant enhancements in the absorption band ( $500\text{-}1060\text{ cm}^{-1}$ ).

### 3.5 Activity of catalysts for water gas shift reaction

The water gas shift reaction was carried out in the temperature range of  $150\text{-}360^\circ\text{C}$ . The catalysts used were  $\text{CeO}_2$  and 20 mol. %  $\text{Cu/CeO}_2$  nanofibers. The experimental procedure and product analysis are already discussed in the experimental section. Initially, the conversion of CO increases with increasing temperatures but then starts decreasing at elevated temperatures, thereby showing a maxima point for all the catalysts. At lower temperatures, there is a large difference in the experimental conversion and corresponding equilibrium conversion. However, at higher temperatures, the conversion slowly approaches the equilibrium conversion. The aforementioned phenomena can be explained by the facts that at lower temperatures, the rate of reaction is low

and the residence time inside the reactor is far below the time required to reach equilibrium conversion. Moreover, the water gas shift reaction is mildly exothermic in nature and hence, the equilibrium conversion is higher at lower temperatures.

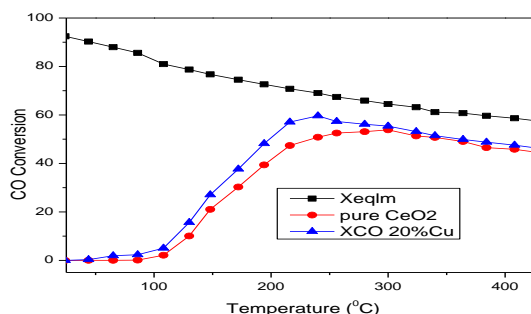


**Fig. 6: Stability of CeO<sub>2</sub> and 20 mol. % Cu/CeO<sub>2</sub> catalyst during WGSR runs in 150-400 °C, feed gas flow rate: 1.5 ml/min. CO, 58.50 ml/min N<sub>2</sub> and water vapors.**

#### IV. CONCLUSION

The electrospun nanofibers of pure CeO<sub>2</sub> and 20 mol. % Cu/CeO<sub>2</sub> were successfully fabricated using Electrospinning technique. The synthesized nanofibers were characterized by SEM and the average diameters of the nanofiber (after calcinations) were found to be in the range between 70 to 100 nm. The nanofibers exhibited characteristic peaks of a fluorite-like cubic phase in the XRD analysis. The most intense peaks of CeO<sub>2</sub> were visible at two-theta values of 28.74° and 47.24°. The average crystallite sizes of calcined pure CeO<sub>2</sub> and 20 mol. % Cu/CeO<sub>2</sub> nanofiber were calculated to be 12 nm and 9 nm (from Debye Scherer formula), respectively. The WGSR was carried out in the temperature range of 150-360°C. 20 mol. % Cu/CeO<sub>2</sub> catalysts showed superior activity than pure ceria catalyst; pure CeO<sub>2</sub> and 20 mol. % Cu/CeO<sub>2</sub> nanofiber exhibited CO conversion efficiencies of around 57% and 61%, respectively.

#### V. ACKNOWLEDGEMENT

The authors thankfully acknowledge IIT (BHU), Varanasi for laboratory facility and the financial support from MHRD, Govt. of India.

#### REFERENCES

- [1] R. T. Watson, Climate change 2001, Synthesis report. Published for the Inter-Gov. Panel on Climate Change IPCC, Cambridge University Press, Cambridge, UK; 2001.
- [2] L. Barreto, A. Makihiro, K. Riahi, Int. J. Hydrogen Energy 28 (2003) 267.
- [3] F. M. Langer, E. Tzimas, M. Kaltschmitt, S. Peteves, Int. J. Hydrogen Energy 32 (2007) 3797.
- [4] W. C. Lattin, V. P. Utgikar, Int. J. Hydrogen Energy 32 (2007) 3230.
- [5] . Eliezer, N. Eliaz, O. N. Senkov, F. H. Froes, Mater. Sci. Eng., A 280 (2000) 220.
- [6] N. Eliaz, D. Eliezer, D. L. Olson, Mater. Sci. Eng., A 289 (2000) 41.
- [7] T. L. Le Valley, A. R. Richard, M. Fan, Int. J. Hydrogen Energy 39 (2014) 16983.

- [8] F. A. de Bruijn, B. Rietveld, R. W. van den Brink, in: G. Centi, A. van Santen (Eds.), *Catalysis for Renewables*, Wiley-VCH, Weinheim, 2007, p. 299.
- [9] R. A. Dagle, Y. Wang, G.G. Xia, J. J. Strohm, J. Holladay, D. R. Palo, *Appl. Catal., A* 326 (2007) 213.
- [10] J.H. Wee, K.Y. Lee, *J. Power Sources* 157 (2006) 128.
- [11] R. J. Farrauto, Y. Liu, W. Ruettinger, O. Ilinich, L. Shore, T. Giroux, *Catal. Rev. Sci. Eng.* 49 (2007) 141.
- [12] M. A. Soria, P. Perez, S. A. C. Carabineiro, F. J. M. Hodar, A. Mendes, L. M. Madeira, *Appl. Catal., A: Gen.* 470 (2014) 45.
- [13] G. C. Pontelli, R. P. Reolon, A. K. Alves, F. A. Berutti, C. P. Bergmann, *Appl. Catal., A: Gen.* 405 (2011) 79.
- [14] P. van de Witte, P. J. Dijkstra, J. W. A. Berg, J. Feijen, *J. Membr. Sci.* 117 (1996) 1.
- [15] S. K. Chakarvarti and J. Vetter, *Radiat. Meas.* 29 (1998) 149.
- [16] W. T. Gibbons, T. H. Liu, K. J. Gaskell, G. S. Jackson, *Appl. Catal., B: Environ.* 160-161 (2014) 465.
- [17] R. Ramaseshan, S. Sundarrajan, R. Jose, S. Ramakrishna, *J. Appl. Phys.* 102 (2007) 111101.
- [18] S. Homaeigohar, M. Elbahri, *Materials* 7 (2014) 1017.
- [19] Z. M. Huang, Y. Z. Zhang, M. Kotaki, S. Ramakrishna, *Compos. Sci. Technol.* 63 (2003) 2223.
- [20] S. Xu, D. Sun, H. Liu, X. Wang, X. Yan, *Catal. Comm.* 12 (2011) 514.